Design of an Adaptive Neuro-Fuzzy Inference Control System for the Unified Power Flow Controller

M. E. A. Farrag BSc MSc PhD MIET MIEEE and G. A. Putrus BSc MSc PhD MIET CEng

Abstract-- This paper presents a new approach to control the operation of the Unified Power Flow Controller (UPFC) based on the Adaptive Neuro-Fuzzy Inference Controller (ANFIC) concept. The training data for the controller is extracted from an analytical model of the transmission system incorporating a UPFC. The operating points' space is dynamically partitioned into two regions: an inner region where the desired operating point can be achieved without violating any of the UPFC constraints; an outer region where it is necessary to operate the UPFC beyond its limits. The controller is designed to achieve the most appropriate operating point based on the real power priority. In this study the authors investigated and analysed the effect of the system short circuit level on the UPFC operating feasible region which defines the limitation of its parameters. In order to illustrate the effectiveness of the control algorithm both simulation and experimental studies have been conducted using MATLAB/SIMULINK and dSPACE DS1103 data acquisition board. The results obtained show a clear agreement between simulation and experimental results which verify the effective performance of the ANFIC controller.

Index terms- Artificial intelligence, Fuzzy, Neural networks, UPFC, Flexible AC transmission systems.

I. NOMENCLATURE

V_{ser}, Series injected voltage
V_{sh}, Shunt injected voltage
V_1, Sending end voltage
V_2, Receiving end voltage
V, Voltage to the right of UPFC
δ, System transmission angle
ΔP, Change in real power
ΔQ, Change in reactive power
β, Relative in-phase series injected voltage
γ, Relative perpendicular series injected voltage
η, Relative in-phase shunt voltage
ξ, Relative perpendicular shunt voltage
P_{ex}, Exchanged real power
Q_{sh}, Shunt reactive power
KX, Short circuit level

II. INTRODUCTION

The Unified Power Flow Controller (UPFC) is the second generation of the Flexible A.C. Transmission Systems (FACTS) devices that is able to provide series and shunt compensations in transmission systems. Since the proposal of the UPFC in 1992 [1], there has been increasing interest in finding a suitable control method to suit a range of system operating conditions [2].

In previous studies, various controllers have been proposed to regulate the operation of the UPFC. Cross-coupling PI controllers are proposed to minimise the interaction between the real and reactive power flow [3]. In addition, the use of de-coupling PI controllers with a predictive internal control loop has also been investigated in order to reduce the effect of harmonics in the current measurement [4]. A hybrid (direct-coupling and cross-coupling) PI controller was suggested to dampen the transient power fluctuation caused by the controller [5]. A common limitation of PI controllers is that they do not always perform satisfactorily over a wide range of operating points. This is caused by the control parameters being determined based on certain system conditions. The robust control theory based on H_∞ has been used in the UPFC controller design [6]. This requires a defined mathematical model of the power system including the UPFC, consequently the required on-line computation to solve the optimisation equations is intensive. Methods based on fuzzy control theory have also been proposed [7]-[9]. In spite of the qualitative approach that allows fast response and stable operation, a drawback of these methods (using fuzzy logic) is that the chosen membership functions are not adapted according to the system operating condition.

An adaptive Neuro-Fuzzy Inference System (ANFIS) combines the fuzzy qualitative approach with the adaptive capabilities of neural networks to achieve improved performance [10]. Compared to a standard fuzzy logic controller, a control system based on this concept can be trained without significant expert knowledge.

For the purpose of this study, the UPFC is modelled as two controllable voltage sources. Each source is split into two orthogonal components that are used to independently regulate the real and reactive power flow in the transmission line by controlling the series part of the UPFC. The bus voltage and real power exchange between the series and shunt inverters is regulated by the shunt part of the UPFC. Hence, four control loops are simultaneously used at every sample to achieve the required control action. In this study, an Adaptive Neuro Fuzzy Inference Controller (ANFIC) is adapted for the UPFC. The training data is generated from the relationship between the change in the real and reactive power and the corresponding UPFC control variables, which can be derived analytically, based on the power system parameters. The control variables are the levels of the inserted voltage components referenced to the system busbar voltage at which the UPFC is connected. When the desired operating point of the power system would cause the UPFC to violate its voltage and / or current limits, the controller responds according to a real-power-priority logic. As a result, the best acceptable

M. E. A. Farrag is with School of Engineering and Computing, Glasgow Caledonian University, Cowcaddens Rd, G4 0BA, UK. mohamed.farrag@gcu.ac.uk.
G. A. Putrus is with the School of Computing, Engineering and Information Sciences, Northumbria University, NE1 8ST, UK ghanim.putrus@unn.ac.uk.

operating point is achieved for the power system while the UPFC remains within its operating limits. The impacts of the system fault level on the system operating area are also analysed. The designed controller is tested using a UPFC computer model in MATLAB/SIMULINK environment. The results illustrate the effectiveness of the proposed controller to achieve the desired performance. Experimental results obtained by implementing the ANFIC on a DSP dSPACE ds1103 data acquisition system are also presented; the experimental results agree with the simulation results.

III. UPFC MODE OF OPERATION AND MODELLING

There are different modes of operation for each of the inverters constituting the UPFC [11]-[13]. In this paper, the following constraints to the modes of operation are considered when designing the UPFC control system:

- For the series compensation inverter, the phase and magnitude of the inserted compensation voltage are controlled so as to maintain or vary the active and reactive power-flow in the transmission line within a predetermined region: this is known as automatic power-flow mode of operation.
- For the shunt inverter, an automatic voltage control mode is considered, i.e. the inverter is operated to absorb or generate certain amounts of reactive power to regulate the bus voltage at which the UPFC is connected.

The single-phase equivalent circuit of a simplified transmission system, including a transmission line and two voltage sources (V_S and V_2), as shown in Fig. 1, is used in the present study. The UPFC is modelled as two controllable voltage sources; V_{ser} represents the series inverter while V_{sh} represents the shunt inverter. Two perpendicular components, one in-phase with the system bus voltage V_1 and the other in quadrature (as shown in Fig. 2), are used to represent both compensation voltages generated by each inverter of the UPFC.

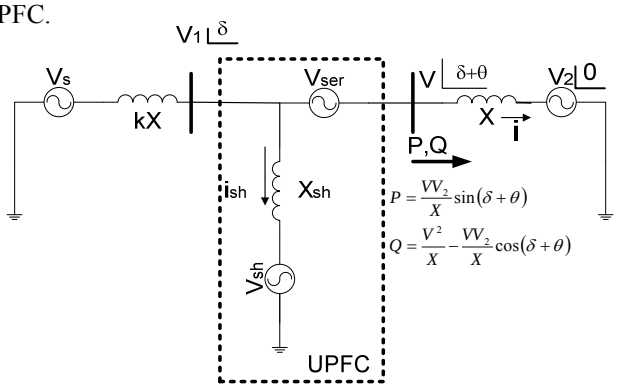

Fig. 1. Power system including a UPFC model

IV. SYSTEM OPERATING REGION

A. *Series Inverter Operating Region*

Considering the effect of the series compensation voltage V_{ser} only, and referring to the phasor diagram given in Fig. 2-a, it can be shown that the per unit change (VA base is $\frac{V_1 V_2}{X}$) of real and reactive power flow as a function of the series inserted voltage components may be expressed as [9].

$$\Delta P = \beta \sin\delta + \gamma \cos\delta \quad (1)$$

$$\Delta Q = \gamma^2 + \gamma \sin\delta + (2 - \cos\delta)\beta + \beta^2 \quad (2)$$

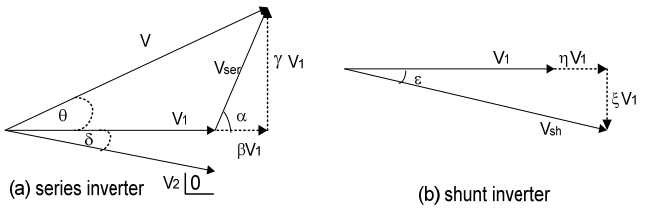

Fig. 2. UPFC Vector diagram

where, β *and* γ are the relative amplitudes of the in-phase and quadrature components of the inserted voltage respectively. δ is the system transmission angle which can be obtained by using on-line state estimation.

The appropriate values of β *and* γ corresponding to the desired change of the real and reactive power may be obtained by solving (1) and (2). Real roots for β *and* γ require the inequality in (3) to be satisfied [9].

$$\Delta P^2 + 2\Delta P \sin\delta - \Delta Q \le 0.25 - \cos\delta + \cos^2\delta \quad (3)$$

This inequality represents the feasible region, assuming an unlimited inserted voltage and an ideal UPFC. The area is characterised by the system transmission angle as shown in Fig. 3, for $\delta = 20^o$ and $\delta = 30^o$.

In practice, as discussed in [14], there are several constraints that limit the UPFC operation:

- VA rating of the series inverter which is determined by the maximum line current and the maximum inserted voltage.
- VA rating of the shunt inverter which is determined by the real and reactive power exchange between the inverter and the a.c. system.
- The line-voltage at the UPFC right-side (V).
- The system short circuit level.

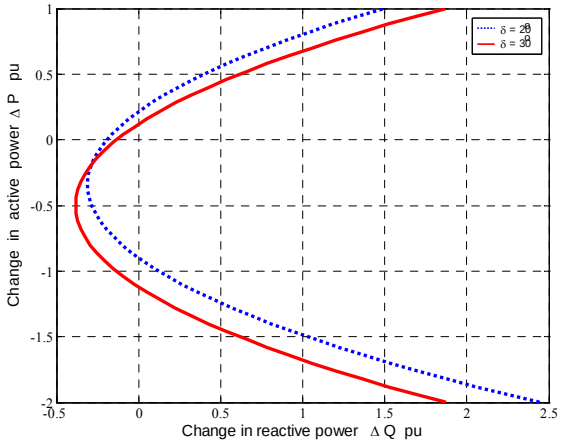

Fig. 3. Global operating area of the UPFC

These limits are determined based on the transmission system topology and power demands. The line-current and line-voltage at the UPFC right-side can be controlled by the

series compensation voltage; therefore, these limits are mainly reflected in the maximum inserted voltage. During operation of the UPFC, before a control limit is exceeded, the controller is required to find an appropriate operating point within the system feasible limits. The solution depends on the system operating conditions, and Neuro-Fuzzy techniques are inherently advantageous in such decision making process. Thus, in this research, the authors investigated the effect of maximum inserted voltage on the system feasible region.

From (1) and (2), the per unit change in real and reactive power in the transmission system can be rewritten as:

$$\Delta P = V_{ser}\sin(\delta+\alpha) \tag{4}$$

$$\Delta Q = V_{ser}^2 - V_{ser}\cos(\delta+\alpha) + 2V_{ser}\cos\alpha \tag{5}$$

Where, $V_{ser} = \sqrt{\beta^2+\gamma^2}V_1$ *and* $\alpha = \tan^{-1}\frac{\gamma}{\beta}$

By eliminating α from (4) and (5), the relationship between the real power deviation ΔP and the reactive power deviation ΔQ in terms of the inserted voltage can be obtained and is shown graphically in Fig. 4. As an example, the cases when $\Delta V_{ser_{max}} = 0.25\ pu$ and $\Delta V_{ser_{max}} = 0.35\ pu$ for a system transmission angle $\delta = 30^o$ are considered. This figure shows that the feasible operating area is defined by the maximum inserted voltage, which is determined by the VA rating of the series inverter. Inside this area it is possible to find a combination of β *and* γ that gives the required real and reactive power. Fig. 4 shows that $\Delta V_{ser_{max}}$ determines the maximum possible per unit change in the real power. Further analysis, conducted by the authors, shows that this occurs when the angle $(\delta+\alpha)$ has a value of $\pi/2$.

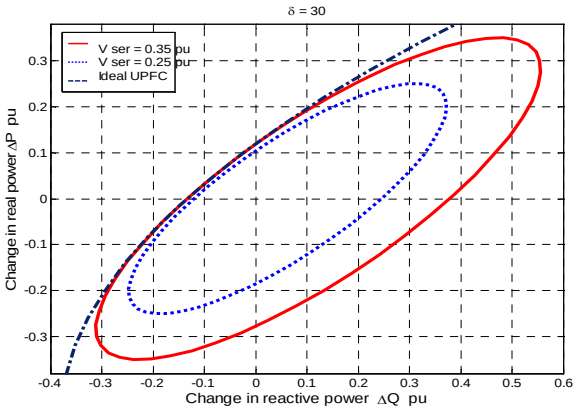

Fig. 4. Restricted operating area of the UPFC

B. Effect of the System Short Circuit Level

The performance of FACTS devices (including the UPFC) depends on the network configuration beyond the bus-bar at which the device is connected. As shown in Fig. 1, the system Short Circuit Level (SCL) is determined by the reactance KX series with the system sending-end voltage V_S. Obviously, the system's fault level decreases as the factor K increases (i.e. the system becomes weak), while a strong system has a small value of K. Referring to the vector diagram given in Fig. 2-a, introducing the system reactance KX into the active and reactive power flow equations (with the assumption that the UPFC shunt part is supporting the system bus voltage such that $|V_s| = |V_1|$) yields,

$$P = \frac{VV_2}{(1+K)X}\sin(\delta+\theta) \tag{6}$$

$$Q = \frac{1}{(1+K)^2 X}\left\{V^2 - VV_2\cos(\delta+\theta)\right\} - \frac{K}{(1+K)^2 X}\left\{V_2^2 - VV_2\cos(\delta+\theta)\right\} \tag{7}$$

Where; $V^2 = V_1^2 + V_{ser}^2 + 2V_1V_{ser}\cos\alpha$,

and $\theta = \tan^{-1}\dfrac{V_{ser}\sin\alpha}{V_1 + V_{ser}\cos\alpha}$

Hence, the effect of the system short circuit level is to reduce the feasible area, as shown in Fig. 5, for K = 0, 0.1 and 0.5.

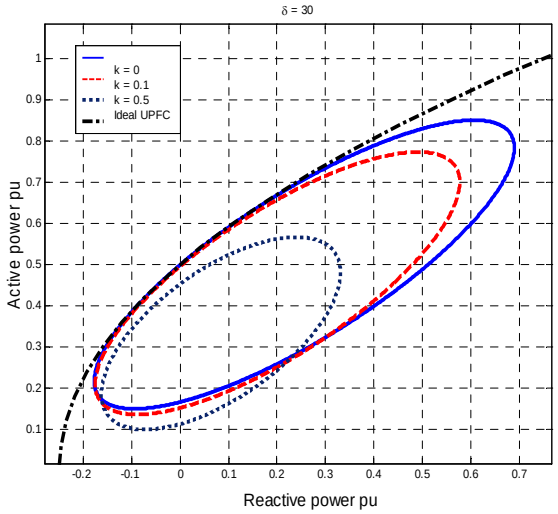

Fig. 5. System feasible region for different SCL.

V. THE ADAPTIVE NEURO-FUZZY INFERENCE SYSTEM (ANFIS)

Fuzzy logic controllers play an important role in many practical applications. However, there are no standard methods for transforming human knowledge into the rule-base of the fuzzy inference system. Hence, the selection of the size, type and parameters of the input and output membership functions has often been achieved via trial and error. There is a real need for effective methods of tuning the membership functions and reducing the rule base to the minimum essential rules.

The Adaptive Neuro-Fuzzy Inference System (ANFIS) was developed to overcome the above difficulties. ANFIS combines the fuzzy qualitative approach with the adaptive learning capabilities of the neural network; hence such a system can be trained without a great amount of expert knowledge usually required for the standard fuzzy logic [15]. As a result, the rule-base can be reduced. A typical architecture of ANFIS based on the first order Takagi-Sugeno model is shown in Fig. 6, with a two-inputs (x, y) and one-output (f) fuzzy system. The architecture is expanded as follows:

Rule ij:

$$if\left(x\,is\,A_i\right)and\left(y\ \ is\ \ B_j\right)then\left(\ f_{ij}=g_{ij}x+h_{ij}y+r_{ij}\right)$$

A_i and B_j represent the linguistic variables of the corresponding input membership functions (MF). $g_{ij},\ h_{ij}\ and\ r_{ij}$ are the parameters of the output membership functions. The parameters of the input and output membership functions are determined during the training stage. ANFIS consists of five layers, each layer has either fixed nodes (that have no parameters to be tuned) represented by a circle or adaptive nodes (that have parameters to be tuned during training) represented by a square as shown in Fig. 6-a, with the inference system presented in Fig. 6-b. The output of the five layers which emulate fuzzy system design steps is given as follows [10].

$$O_{1i}=\mu_{A_i}\left(x\right)\ \text{or}\ O_{1j}=\mu_{B_j}\left(y\right) \tag{8}$$

$$O_{2_{ij}}=W_{ij}=\mu_{A_i}\left(x\right)\mu_{B_j}\left(y\right),i=1,2,\ldots N,j=1,2,\ldots M \tag{9}$$

$$O_{3_{ij}}=\bar{W}_{ij}=\frac{W_{ij}}{\sum_{\forall i,j}W_{ij}} \tag{10}$$

$$O_{4_{ij}}=\bar{W}_{ij}f_{ij}=\bar{W}_{ij}\left(g_{ij}x+h_{ij}y+r_{ij}\right) \tag{11}$$

$$O_5=f=\sum_{\forall i,j}\bar{W}_{ij}f_{ij}=\sum_{\forall i,j}\frac{W_{ij}f_{ij}}{\sum_{\forall i,j}W_{ij}}=\frac{\sum_{\forall i,j}W_{ij}f_{ij}}{\sum_{\forall i,j}W_{ij}} \tag{12}$$

The objective of the learning algorithm is to adjust all these parameters to make the ANFIS output best match the training data. A hybrid learning strategy (Gradient Descent GD and Least Squares Estimate LSE) can be applied to identify the network parameters. The GD method is used to update the antecedent membership function parameters and the LSE method is used to identify the consequent parameters.

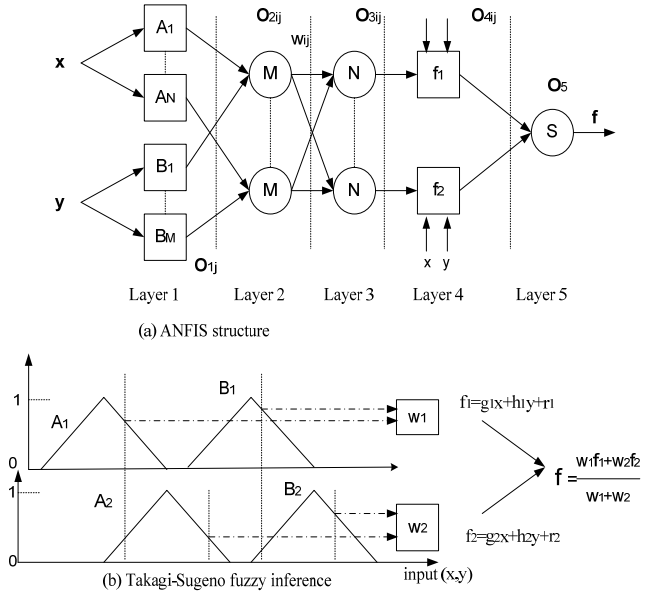

Fig. 6. ANFIC layout

VI. ADAPTIVE NEURO- FUZZY INFERENCE CONTROL (ANFIC) OF THE UPFC SERIES INVERTER

As shown in Fig. 6, the ANFIC is based on the first order Takagi–Sugeno model and allows only a single output. ANFIC has been used to train the gain-scheduling controller for a power system [16]. Five Linear Quadratic Regulator (LQR) controllers have been designed and the ANFIC controller is trained to choose the most suitable controller depending on the current system operating point. As discussed in section IV, the series part of the UPFC system used in the present study has two control variables $\beta\ and\ \gamma$ to control the real and reactive power flow. This implementation therefore requires the design of two independent fuzzy systems, one for each control variable. Both systems have the same inputs $\left(\Delta P,\Delta Q\right)$ and the same structure.

A. Training Data Generation

To train the ANFIC, there is a need to generate two sets of data: input data and the corresponding output data. The training input data are two vectors of the deviation in real power $\left(\Delta P\right)$ and the deviation in the reactive power $\left(\Delta Q\right)$ within the system feasible region. The training output data are the two components of the corresponding series inserted voltage $\beta\ and\ \gamma$.

By re-arranging (1) and (2), the inserted voltage control parameters $\beta\ and\ \gamma$ may be obtained as a function of the changes in the real and reactive power flow in the transmission line.

$$\gamma=\frac{\left(\Delta P-\sin\delta\right)}{\cos\delta} \tag{13}$$

$$\beta=\min\left(\left|\frac{-b\pm\sqrt{b^2-4ac}}{2a}\right|\right) \tag{14}$$

Where, $a=1$, $b=2cos^2\delta-\cos\delta-2\Delta P\sin\delta$ and $c=\Delta P^2+\Delta P\sin\delta\cos\delta-\Delta Qcos^2\delta$

The training data for $\beta\ and\ \gamma$ can be generated for the required maximum inserted voltage. The values are independent of the transmission line reactance as $\left(\Delta P\ and\ \Delta Q\right)$ are expressed in per unit based on $\frac{V_1V_2}{X}$.

B. Real Power Priority

During normal operation, the power system operating point falls within the defined feasible region. During certain operating conditions, the system desired operating point might fall outside the feasible region defined by the UPFC capabilities given in Fig. 4. In this case, the inserted voltage of the series inverter would exceed its design limit. The system controller is required to move to a new operating point to avoid such violation. As shown in Fig. 7, the new operating point must be within the feasible region circumference, which satisfies the maximum inserted voltage. The exact operating point may be chosen according to the reactive power priority or real power priority.

In the first case, the angle of the inserted voltage is obtained such that the reactive power is identical to the requested value regardless of the real power. Because of the reactive power support capability of the UPFC shunt inverter, the second approach (i.e. real power priority) is considered here to determine a suitable operating point. Therefore, the angle of the inserted voltage is changed until the real power reaches the required value of the maximum achievable $\Delta\hat{P}$. This angle can be calculated by using (4).

Referring to Fig. 7, the required change of active power is:

$$\Delta\hat{P} = V_{ser}\sin\left(\delta + \hat{\alpha}\right) \tag{15}$$

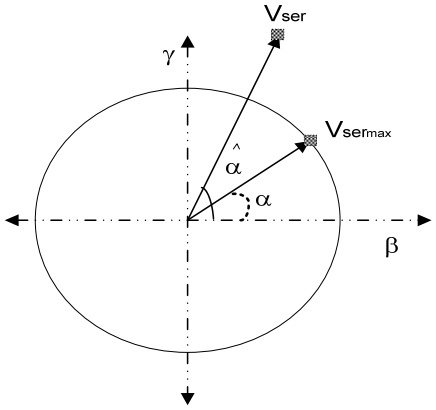

Fig. 7. Injected angle under real power priority

By equating the change in real power in (15) and (4) for $V_{ser} = V_{ser_{max}}$, the required angle can be found as:

$$\alpha = -\delta + \sin^{-1}\left\{\frac{V_{ser}}{V_{ser_{max}}}\sin\left(\delta + \hat{\alpha}\right)\right\} \tag{16}$$

Based on this analysis, the values of the control variables defined by (13) and (14) are updated to include the uncontrolled region when it is beyond the UPFC capability to follow the desired changes in real and/or reactive power.

C. ANFIC Training

The training data are based on (13) – (16). The tuning algorithm discussed in section V is used to modify the premise and consequent parameters of the Neuro-Fuzzy network (shown in Fig. 6) to match the training data. Each input range is initially partitioned into 11 triangular MF's with a 50% overlap. Therefore, 121 rules for each control variable are obtained. The training procedure in this research is achieved by using MATLAB / FUZZY Logic Toolbox. The Mean Square Error (MSE) between the target values of each control variable and the trained ANFIC output is relatively small as shown in Fig. 8, for β *and* γ.

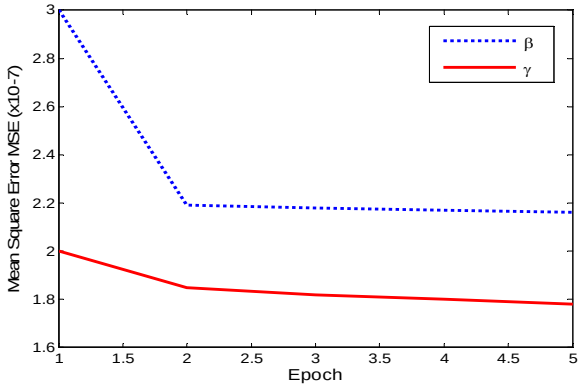

Fig. 8. Mean Square Error (MSE) for trained control variables

A test data set (different from training data) is generated to validate the ANFIC learning algorithm for each control variable. Fig. 9, shows the output of the ANFIC, driven by the validation data and the target of the control variables β *and* γ. It is clear that the trained ANFIC gives interpolated results very close to the target at non-trained pairs, as the MSE over the whole tested set is 4.8e-4 and 1.7e-4 for β *and* γ respectively.

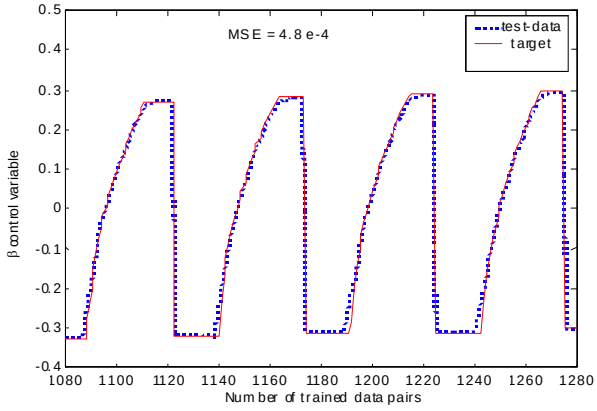

(a) Validation test for β

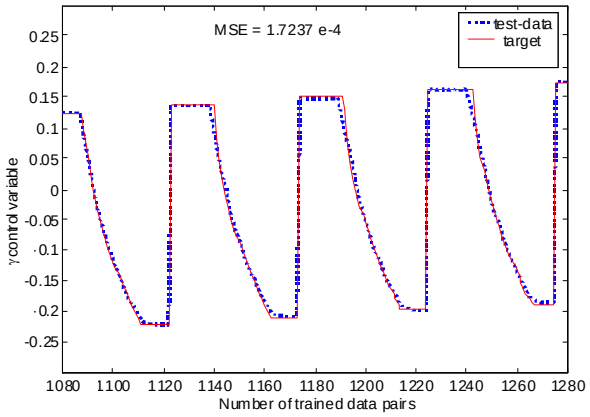

(b) Validation test for γ.

Fig. 9. ANFIC validation for both β and γ

VII. CONTROL OF THE SHUNT INVERTER

The function of the shunt part of the UPFC is to supply the real power demand of the series inverter and to support the system bus voltage. With reference to Fig. 2-b, the real and reactive power flow of the shunt branch can be derived as:

$$P_{sh} = \frac{V_1^2}{X_{sh}}\xi \tag{17}$$

$$Q_{sh} = -\frac{V_1^2}{X_{sh}}\eta \tag{18}$$

Where, η *and* ξ are the in-phase and quadrature components of the shunt inverter output voltage with respect to V_1.

The active power demand of the series inverter should be within the rating of the shunt inverter. The difference between the VA rating of the shunt inverter and the real power demand of the series inverter can be used to exchange the reactive power with the transmission system in order to enhance the UPFC voltage control capability.

By re-arranging (17) and (18), the control parameters of the shunt inverter η *and* ξ may be obtained as:

$$\xi = \frac{X_{sh}}{V_1^2} P_{ex} \tag{19}$$

$$\eta = -\frac{X_{sh}}{V_1^2} Q_{sh} \tag{20}$$

Where, $P_{ex} = P_{sh}$ is the real power exchanged between the series inverter and the a.c. system.

It is clear from (19) and (20) that there is a direct relationship between the shunt inverter voltage components η *and* ξ and (Q_{sh} and P_{ex}) respectively. In order to increase the shunt inverter controller sensitivity the error signal produced by P_{ex} or P_{sh} is used to define the quadrature control signal ξ; this will indirectly guarantee the stability of the dc link voltage. The bus voltage deviation from its set point is used to define the in-phase component η. In this work, a Fuzzy like PI controller (a controller created from fuzzy rules but behaves like a standard PI controller) is used to control the operation of the shunt inverter [9].

VIII. SYSTEM SIMULATION

The system shown in Fig. 1 is simulated in MATLAB, in order to investigate the performance of the suggested ANFIC to regulate the UPFC under different operating conditions (V_1, V_2 *and* X *are* $1\,pu, X_{sh} = 0.15\,pu$). Two cases are described here to illustrate the capability of the UPFC to independently control the active and reactive power flow in the transmission line. A PI controller is used in each case for assessment of the proposed ANFIC controller and the PI control parameters are designed in order to limit the maximum overshot during the transient period and to reduce the interaction between the real and reactive power control loops.

Case 1- In this case the set (desired) and the actual operating points are always inside the feasible control area. The system is tested for two different short circuit levels, as shown in Fig. 10. The system is controlled to make a step change in the reactive power while keeping the active power constant. The active power is then subjected to a step change while the reactive power is fixed. It is obvious from the simulation results that the proposed controller shows good performance in independently controlling the real and reactive power flow. The system response when using the Nuero-Fuzzy controller is almost identical to the PI controller in achieving the real power level and reducing the interaction between the active and reactive power flow, in particular for the active power control loop. Comparing the response in the two graphs, the ANFIC speed of response is less sensitive to the change in the system fault level, while the PI controller has a slightly slower response for low short circuit levels. This can be modified by choosing appropriate gains. The figure also shows the capability of the UPFC to regulate the bus voltage at which the shunt inverter is connected regardless of the controller type for the shunt inverter

Case 2- In this case study, the behaviour of the controller is tested when the design rules are violated. The desired and actual system operating points considered in this case are shown in Fig. 11, where points 1 and 3 are located inside the controlled region while points 2 and 4 are outside. Based on the training criteria, the ANFIC controller moves the operating point from outside the feasible operating area to the circumference of the area based on the real power priority. As discussed in section VI (B), the operating points which are outside the feasible area are included in the training data set of ANFIC. Therefore, the controller response is inherently optimised; that is, it changes the reactive power whilst keeping the real power at the desired level as well as maintaining the

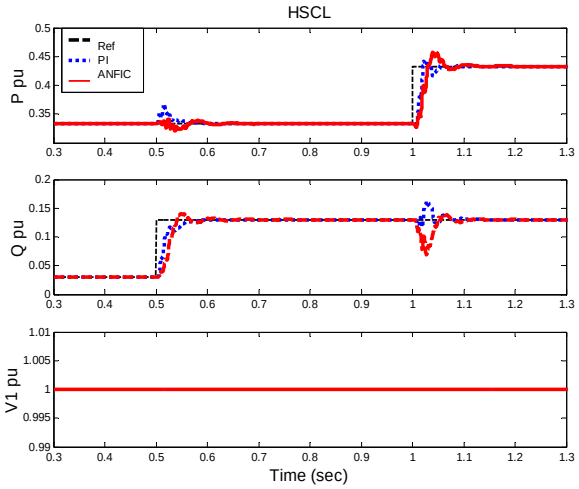

(a) System's response for high short circuit level

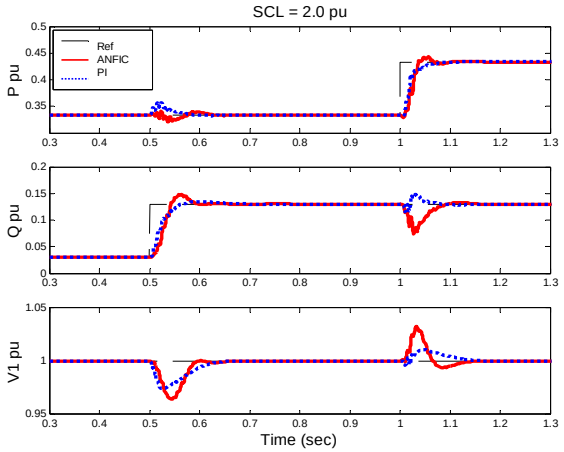

(b) System's response for low short circuit level

Fig. 10. System's response for two short circuit levels

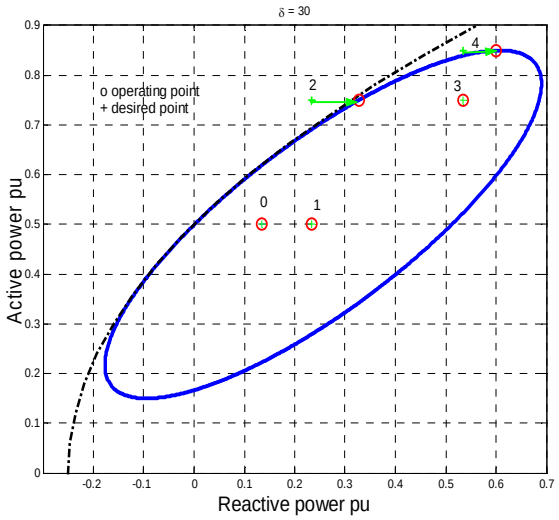

Fig. 11. System set-points and actual operating points

bus voltage constant, as shown in Fig. 12–a. It is clear that the PI controller makes the system converges to an undesired steady-state point, especially for the active power control loop. This new state is determined only by the limit of the magnitude of the injected voltage components. It is also clear from Fig. 12, that the PI controller produce a long converge time from point 2 to the desired operating point 3 which is located inside the feasible region. In order to clarify the capability of the PI controller and to obtain a fair assessment of the ANFIC controller, a power flow optimiser is designed for the PI controller to give it the ability to choose the best acceptable operating point when the system limits are violated. This is shown in Fig. 12-b, where the operation of ANFIC and optimised PI controllers are almost identical.

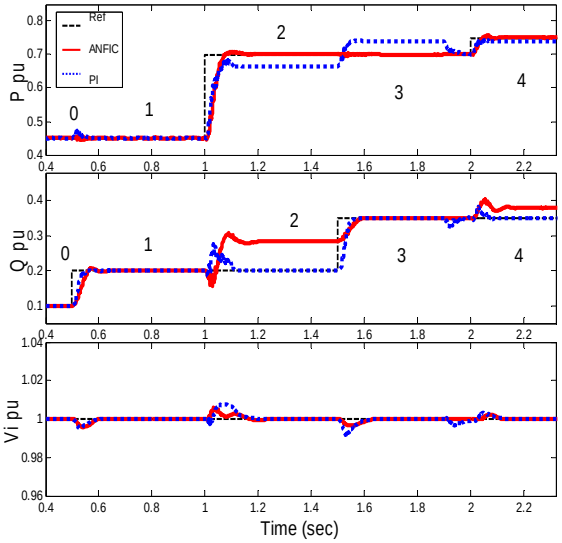

(a) System's response with ANFIC and un-optimised PI

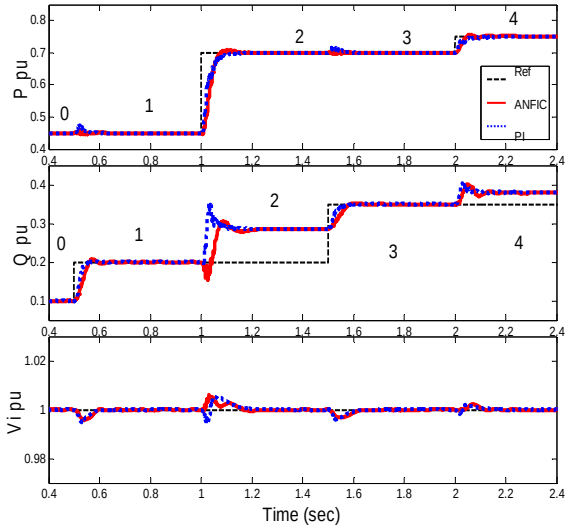

(b) System's response with ANFIC and optimised PI

Fig. 12. System response when the system is subjected to constraints violations

IX. EXPERIMENTAL RESULTS

The laboratory test rig of a simplified transmission system incorporating a UPFC used in this work is shown in Fig. 13. This is similar to the system given in [17] with the exception that, in this study, the shunt inverter is controlled to support the bus voltage and maintain the d.c. link voltage at a constant level. In [17], a shunt rectifier is used to maintain the d.c. link voltage, which means that only the UPFC series inverter capability is investigated. The system parameters are V_{1LL} = 50 V, f_o = 50 Hz, X/R = 8.76, C = 1000uF and V_{dc} = 80 V. In the experimental model, V_1 and V_2 are the voltages at the sending and receiving ends of the transmission line, respectively. Each inverter is a 6-pulse PWM inverter and connected to the a.c. system through an appropriate transformer. The switching frequency of both inverters is set to 9 times the system frequency in order to eliminate both the even and triplen harmonics.

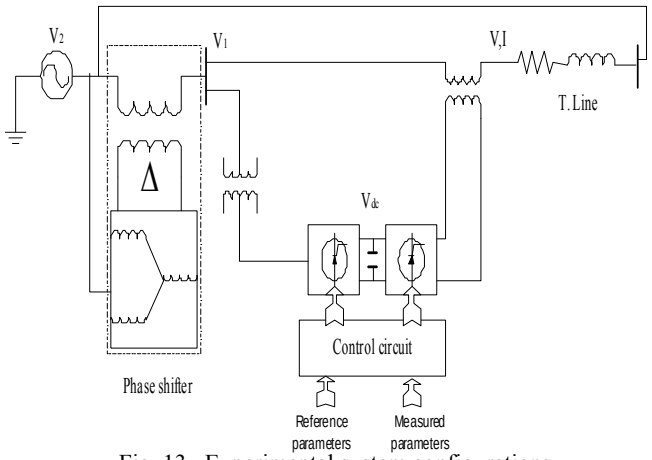

Fig. 13. Experimental system configurations

A phase shifting transformer, which consists of a three-phase transformer and a three-phase slider regulator is employed to simulate a difference in the phase angle between V_1 and V_2. The phase shifting transformer injects a 90^o leading voltage with respect to V_2, and the phase angle of V_1 is set to 6^o. A block diagram of the test setup is shown in Fig. 14.

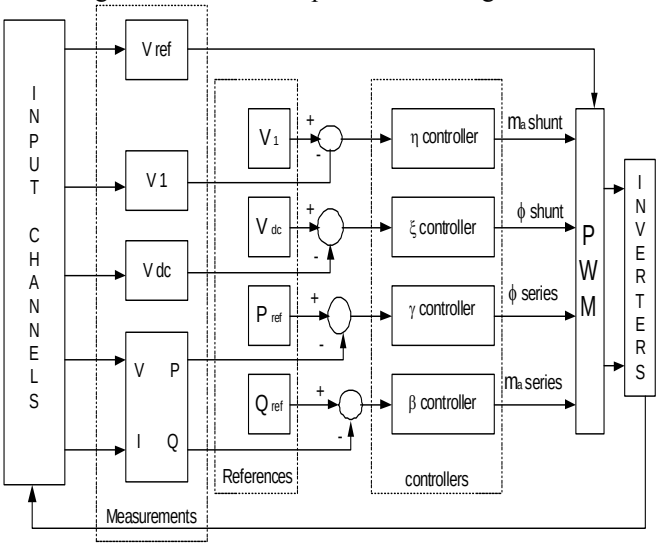

Fig. 14. Block diagram of the practical system

In this study, the controllers are designed in MATLAB/SIMULINK and the host computer is interfaced with the UPFC experimental set-up through the ControlDesk software of dSPACE ds1103 data acquisition board. ControlDesk provides the functions to download the controller to the data acquisition board, to monitor and automate the experiments on real time bases. The dS1103 is a single data acquisition board with DSP slave processor [18].

To match the real time implementation of the ANFIC controller, a step size of 1/ (8*9*50) (i.e. 277.77 e-6 Sec – 8 samples per switching cycle) is chosen as the sampling period of the input and output signals. This is chosen to avoid asynchronisation of the generated PWM. To reduce the computation time of the ANFIC algorithm, the controller inputs are designed to have only 7 membership functions for each input. The shunt controller's parameters are adjusted by using first order Takagi-Sugeno Fuzzy-like-PI controllers. The three-phase PWM generator of the slave DSP on the main board (dSPACE ds 1103) generates the PWM for the series inverter. The shunt inverter switching pattern is obtained by three single-phase PWM generators on the main board.

Fig. 15, shows the experimental waveforms for a step change in active and reactive power flow. It is clear from the results that the UPFC controlled by a PI controller or the ANFIC algorithm is capable of independently controlling the active and reactive power, in addition to controlling the dc link and supporting the system bus voltage. The response of the PI controller is slow and requires adequate on-line tuning of its gains (proportional and integral). However, this is not the case for the ANFIC as it is already trained to provide optimal response without gain adjustment.

X. CONCLUSIONS

In this paper, an Adaptive Neuro-Fuzzy Inference Controller (ANFIC) is proposed to control the series part of the UPFC based on the relationship between the required power flow and the inserted voltage components. The space of training data was partitioned into two regions. The inner region satisfies the limit of the VA rating of the UPFC inverter. The outer region represents the UPFC control variables when it exceeds the limits of operation. The effect of the system short circuit level on the operating feasible region has been investigated. Different scenarios have been studied to demonstrate the capability of the UPFC to independently control the real and reactive power flow. The robustness of the proposed controller has been evaluated for a wide range of operating conditions, including those which are possible in actual systems (e.g. 10-20% change in power flow) and other extreme cases which may occur under abnormal conditions. Simulation and experimental results show that the ANFIC controller can perform better than a PI controller for different operating conditions regardless of the location of the operating

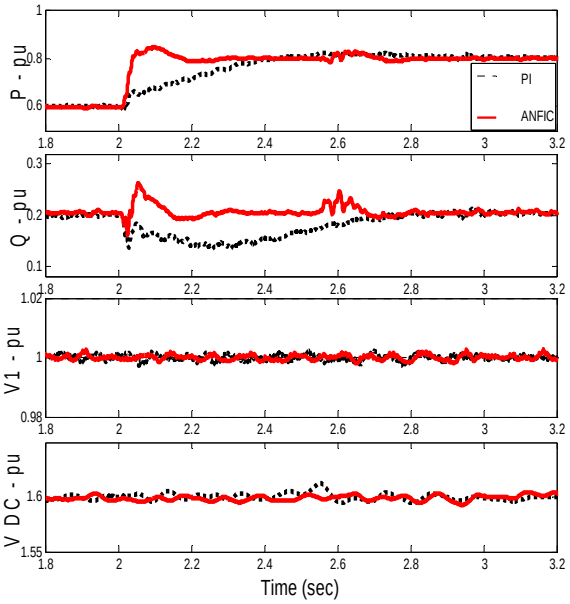

(a) System's response for a step change in active power

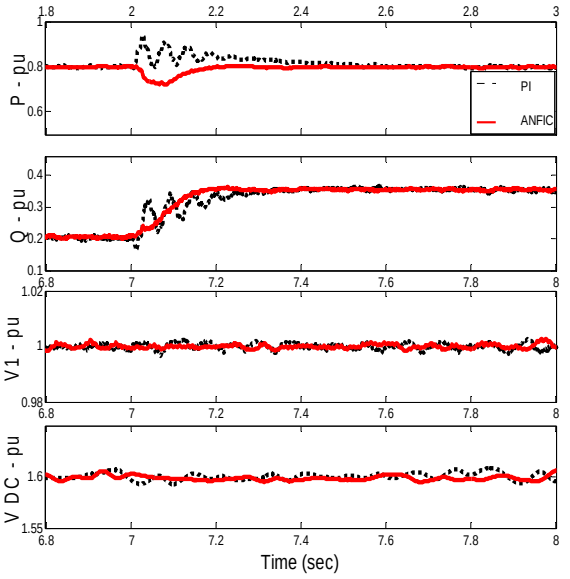

(b) System's response for a step change in reactive power

Fig. 15. Experimental results

points (inside or outside the operating area). Also, the ANFIC controller minimises the interaction between the real and reactive power flow. The real power priority concept is introduced in this paper to define the most appropriate operating point when system limits are violated. The analytical procedures presented in this paper are verified by simulation and experimental work. The results presented show a good agreement between the experimental and simulation results.

XI. REFERENCES

[1] L. Gyugyi, A unified power flow control: concept for flexible ac transmission systems, IEE Proceeding C, Vol. 139 (4) (1992) pp. 323-331.

[2] K.R. Padiyar, K. UmaRao, Modelling and control of unified power flow controller for transient stability, Electrical Power & Energy Systems, 21 (1999) pp. 1-11.

[3] Q. Yu, et al, Investigation of dynamic controllers for a unified power flow controller, IEEE 22nd Int. Conf. On Industrial Electronics, Control and Instrumentation, IECON, Taiwan, Aug. (1996), pp. 1764-1769.

[4] P. Papic, et al, Basic control of unified power flow controller, IEEE Transactions on Power Systems, Vol. 12 (4) (1997), pp. 1734-1739.

[5] H. Fujita, Y. Watanabe, H. Akagi, Control and analysis of a unified power flow controller, IEEE Transactions on Power Electronics, Vol. 14 (6) (1999), pp. 1021-127.

[6] M. Vilathgamuwa, et al, A synchronous reference frame based control of a unified power flow controller, Int. Conf. On Power Electronics and Drive Systems, Vol. 2 (1997), pp.844-849.

[7] K.Sreenvasachar, S. Jayaram, M.M.A. Salama, Intelligent autonomous control of a unified power flow controller, Int. Conf. On Power Electronics and Drive Systems, Vol. 2 (1997), pp.862-868.

[8] S. Mishra, P.K. Dash, G. Panda, TS –fuzzy controller for UPFC in a multimachine power system, IEE Proc. Gener. Transm. Distrib, Vol. 147 (1) (2000), pp.15-22.

[9] M.E.A. Farrag, G.A. Putrus, L. Ran, advanced control of the unified power flow controller, UPEC'1999, Leicester, Vol. 1 (1999), pp 74-77.

[10] J. Shing, R. Jang, ANFIS: adaptive network-based fuzzy inference system, IEEE Transactions on System Man and Cybernetics, Vol. 23 (3) (1993), pp.665-685.

[11] A. Edris, et al., Controlling the flow of real and reactive power, IEEE Computer Applications in Power, January (1998) pp. 20-25.

[12] S.A. Taher, A.A. Abrishami, UPFC location and performance analysis in deregulated power system, Mathematical problem in Engineering, VCol. 2009, Article ID 109501, 20 pages, 2009.

[13] A. Kumar, S. Chanana, DC model of UPFC and its use in competitive electricity market for loadability enhancement, Proceedings of World Congress on Engineering and Computer Science, Oct. 22-24, San Francisco, USA, 2008.

[14] J.Y. Liu, Y.H. Song, Determining maximum regulating capability of UPFC based on predicting feasibility limit of power systems, Electric Machines and Power Systems, 20 (1998), pp.789-800.

[15] J.J. Bukley, Theory of fuzzy controllers, Fuzzy Sets and Systems, Vol. 51, (1992), pp. 249-258.

[16] F.A. Alturki, A. Abdennour, Design and simplification of adaptive neuro-fuzzy inference controllers for power plants, Electrical Power & Energy Systems, Vol. 21 (1999), pp. 465-474.

[17] H. Fujita, Y. Watanabe, H. Akagi, Transient analysis of a unified power flow controller and its application to design of the dc-link capacitor, IEEE Trans. On Power Electronics, Vol. 16 (5) (2001), pp. 735-740.

[18] DSPACE -ds1103 controller board "features reference" Jan. 2001.

XII. BIOGRAPHIES

Mohamed Farrag (M'1999) was born in Assiut, Egypt, 1967. He received BSc and MSc from the Faculty of Electronics Engineering, Menoufia University, Egypt in 1990 and 1996 respectively, and PhD from Northumbria University, Newcastle, UK in 2002. He was a Lecturer of Electrical Engineering in the Faculty of Industrial Education, Helwan University, Egypt between 2003 and 2007, he joined Northumbria University as a Visiting Lecturer for 2008 then joined Institute of Energy and Sustainable Development, De Montfort University, UK as research fellow. Now he is with Department of Energy Systems Engineering, School of Engineering and Computing, Glasgow Caledonian University, He is engaged in research of power system control and operation, renewable energy and sustainability.

Ghanim Putrus is a Reader in Electrical Power Engineering and Director of Training Programmes for Industry at the School of Computing, Engineering and Information Sciences, Northumbria University, Newcastle upon Tyne, UK. He leads the Power and Wind Energy Research (PaWER) group. Ghanim joined Northumbria University as a senior Lecturer in January 1995, after studying and working at UMIST, Manchester, UK 1986-1990 and 1993-1995. He has over 20 years of teaching and research experience in Electrical Engineering, particularly in the application of power electronics in power systems. He has 72 publications, including one patent, 12 Journal papers and 38 referred conference publications in addition to 19 invited talks at national and international events. He has supervised 12 PhD research projects in the areas of FACTS, custom power technology, power quality and active control of power distribution networks.